

SIMULATION RESULTS OF CURRENT FILAMENTATION INSTABILITY GENERATED FROM PWFA ELECTRON BEAM

B. Allen[#], P. Muggli, University of Southern California, Los Angeles, CA 90089, USA

V. E. Yakimenko, Brookhaven National Laboratory, Upton, NY 11973, USA

T. Katsouleas, Duke University, Durham, NC 27708, USA

C. Huang, University of California Los Angeles, Los Angeles, CA 90024, USA

Abstract

Current Filamentation Instability, CFI, is of central importance for relativistic beams in plasmas for the laboratory, ex. fast-igniter concept for inertial confinement fusion, and astrophysics, ex. gamma ray bursts. Simulations, with the particle-in-cell code QuickPIC, with a beam produced by an RF accelerator and a capillary plasma discharge show the appearance and effects of CFI. The instability is investigated as a function of electron beam parameters (including charge and emittance) and plasma parameters (density and length) by evaluating the beam density and magnetic energy. We present simulation results, discuss further simulation refinements, suggest criteria and threshold parameters for observing the presence of CFI and outline a potential future experiment.

INTRODUCTION

Particle beam transport in plasmas is subject to Current Filamentation Instability (CFI) and results in the breakup of the beam into narrow, high current filaments that enhance the magnetic fields. CFI is a basic plasma instability and is purely transverse electromagnetic. CFI could play a role in the generation of the afterglow observed from Gamma Ray Bursts (GRB's) as well as potentially affect the energy transport in the Fast Igniter - Inertial Confinement Fusion (ICF) concept.

GRB's: The phenomena which create GRB's, their afterglow and the associated magnetic fields is unknown. The Fireball theory [1], which could describe the phenomena causing the afterglow, proposes that the afterglow is generated by relativistic collisionless shocks of electrons, positrons and ions as they travel through the interstellar medium. The energy spectrum of GRB's exhibit jitter radiation, which is radiation produced by synchrotron radiation in random tangled magnetic fields. CFI is one possible source for the magnetic field.

Fast Igniter-Inertial Confinement Fusion [2]: This ICF concept breaks the fusion ignition process into two separate processes. After the pellet is symmetrically compressed with laser beams, a single high intensity ultra short laser pulse impinges on the pellet. When the pulse reaches the critical plasma density the laser energy is converted to hot electrons that transport their energy to the core of the pellet and ignite the fusion process. If CFI occurs the trajectories of the electrons could be affected by the CFI generated magnetic fields and change the

amount of energy deposited and its location.

The beam and plasma conditions under which CFI occurs are 1) the beam is relativistic, 2) the transverse beam size (σ_r) is greater than the collisionless skin depth (c/ω_{pe} , c is the speed of light in vacuum and ω_{pe} is the angular frequency of the plasma) and 3) a large beam density, n_b . The growth rate of the instability scales with the beam density as given by the expression [3]: $\Gamma = \beta_o(\alpha/\gamma_o)^{1/2}\omega_{pe}$ or $\Gamma = \beta_o\omega_{pb}\gamma_o^{-1/2}$ where $\omega_{pe} = (n_e e^2/\epsilon_0 m_e)^{1/2}$, $\omega_{pb} = (n_b e^2/\epsilon_0 m_e)^{1/2}$, $\alpha = n_b / n_e$ and n_e is the plasma density.

SIMULATION SETUP

The BNL-Accelerator Test Facility (ATF) provides independent and well controlled access to the beam and plasma parameters. The ATF beam and plasma parameters are shown in Table 1 [4]. Simulations were conducted with the particle-in-cell code QuickPIC [5]. The simulation model used, Fig. 1, consists of a tri-Gaussian electron beam focused at the entrance of a uniform density plasma of length L_p . Note that with the parameters of Table 1 the beam beta function is 1.17 m, which is much longer than the plasma length (1 – 2 cm). The beam at the plasma exit location therefore looks identical to that at the plasma entrance when the plasma is off.

Table 1: ATF Beam and Plasma Parameters

Parameter	Value
Charge – Q (pC)	150 - 200
Beam Transverse Size – σ_r (μm)	100 - 200
Bunch Length – σ_z (fs)	100
Beam Density – n_b (cm^{-3})	$\sim 10^{14}$
Energy (MeV)	59
Normalized Emittance – $\epsilon_{x,y}$ (mm-mrad)	1 – 2
Plasma Density – n_e (cm^{-3})	$10^{14} - 10^{18}$
Plasma Capillary Length – L_p (cm)	1 and 2

[#]brianall@usc.edu

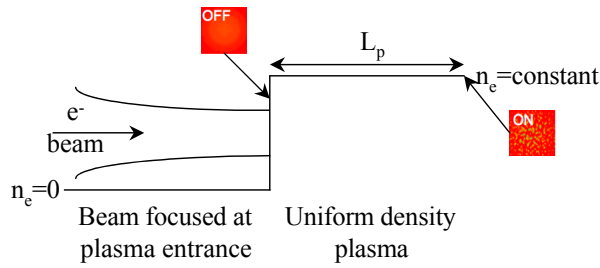


Figure 1: Simulation model. Gaussian distributed electron beam focused at the entrance to a uniform density plasma of length L_p .

BEAM FILAMENTATION

Calculations with growth rate expression and the ATF parameters yield $\Gamma \sim 3.5\text{mm}$, suggesting that filamentation should occur in centimeter long plasmas. Simulations with the parameters in Table 1 initially show (0 cm) a Gaussian distribution at the entrance to the plasma, Fig. 2. After 2 cm of propagation filaments are present with a size $\sim 4\mu\text{m}$ and spacing $\sim 20\mu\text{m}$, both which are on the order of the plasma skin depth, c/ω_{pe} .

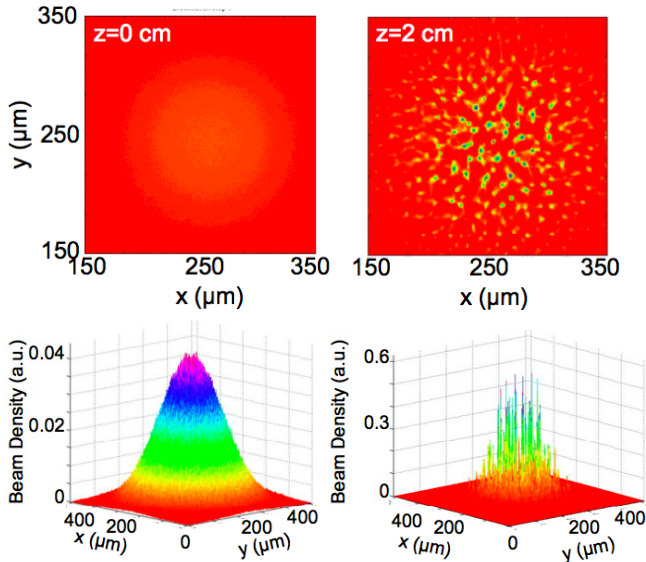


Figure 2: Top: Transverse beam density at (left) 0 cm and (right) 2 cm; Bottom: 3-D beam density for (left) 0 cm and (right) 2 cm. Simulation parameters are listed in Table 1.

CFI GROWTH RATE

The CFI generates enhanced magnetic fields as it grows and the resulting magnetic energy ($\int B_{\text{perp}}^2 dv$) can be used to characterize the growth of the instability. By varying the beam density (through the charge in the beam while holding all other parameters constant) the resulting growth rates were calculated. The growth rates were

extracted from the exponential fit to the semi-log plot of the magnetic energy to the propagation distance. Simulations show, Fig. 3, that the growth rate increases with increased beam density. The growth rate from these simulations show that for the case with the ATF parameters (charge = 200 pC) $\Gamma \sim 3.8\text{mm}$, which compares well with the growth rate from the expression above. Figure 3 also shows that after 2 cm of plasma the magnetic energy has almost reached its saturation volume. The instability may also be partially visible after 1 cm of plasma.

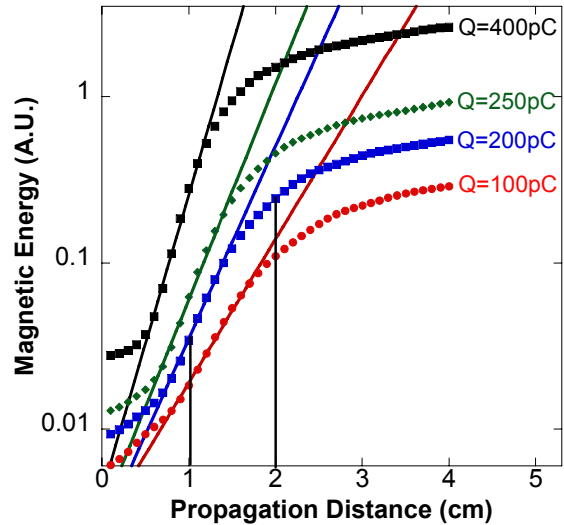


Figure 3: Growth rate of CFI characterized by the magnetic energy for different beam charges and therefore beam density. Straight lines are the fit to the exponential portion of magnetic energy curves. The growth rates are: $\Gamma \sim 2.4\text{ mm}$ ($Q=400\text{ pC}$), $\Gamma \sim 3.4\text{ mm}$ ($Q=250\text{ pC}$), $\Gamma \sim 3.8\text{ mm}$ ($Q=200\text{ pC}$), $\Gamma \sim 5.0\text{ mm}$ ($Q=100\text{ pC}$)

BEAM EMITTANCE EFFECT

The beam emittance competes with the growth of the CFI [6]. This is because the emittance increases the transverse beam size while the growth of the CFI focuses and filaments the beam. By varying the emittance of the electron beam in the simulations and holding all other parameters constant we see that the growth rate is significantly reduced at larger beam emittance, Fig. 4. The emittance with the ATF electron beam is consistently measured between 1 and 2 mm-mrad and is sufficiently low for the CFI to be observed over a plasma length of 2 cm.

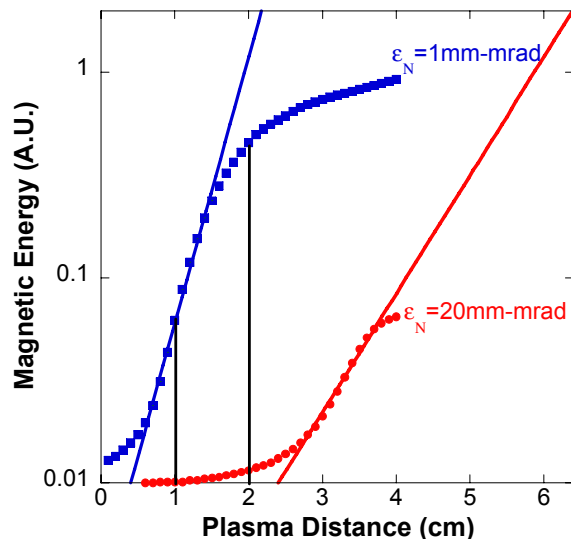


Figure 4: Growth rate of CFI characterized by the magnetic energy for different beam emittance. Straight lines are the fit to the exponential portion of magnetic energy curves. The growth rates are: $\Gamma \sim 3.4$ mm ($\epsilon_N=1$ mm-mrd), $\Gamma \sim 7.5$ mm ($\epsilon_N=20$ mm-mrd).

PLASMA DENSITY EFFECT

Plasma density plays a role in CFI that manifests itself through the collisionless skin depth (c/ω_{pe}). The filaments size and spacing are on the order of the skin depth and therefore scale with $n_e^{-1/2}$. If the plasma density is reduced this leads to larger filament size and spacing. This relationship is observed in simulations, Fig. 5: when the density is decreased from 5×10^{17} to 2.5×10^{17} cm^{-3} the filament size grows from 4 to 6 μm , which fits with the $n_e^{-1/2}$ scaling.

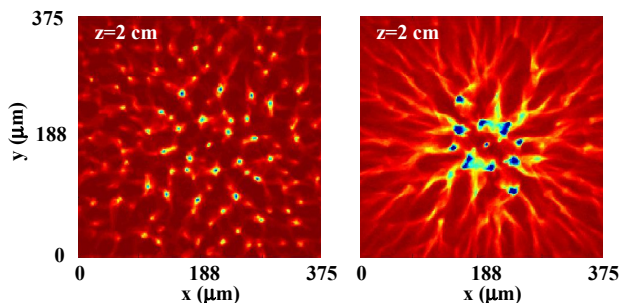


Figure 5: Transverse beam density at 2 cm of plasma propagation for (left) $n_e = 5 \times 10^{17}$ cm^{-3} (right) $n_e = 2.5 \times 10^{17}$ cm^{-3} . Filament size increased from 4 to 6 μm .

CONCLUSION

The beam parameters used in the simulations are available at the ATF. A H_2 plasma capillary discharge [7] that generates plasmas of 1 and 2 cm long is also available. The plasma density at the time when the beam travels into the plasma can be adjusted in the 10^{17} to 10^{18} cm^{-3} range. The simulations presented here show a growth rate for the CFI in good agreement with the one obtained from the analytical expression and show that the CFI should be unambiguously observed at the ATF. Images of the beam at the plasma exit will be acquired that will be similar to these obtained in the simulation, Fig. 2, and show the beam filaments, their size and spacing. In addition we will look for the radiation that is associated with the motion of the electron beam in the CFI generated magnetic fields. The appearance of this radiation is expected to coincide with the appearance of the filaments. The amount of radiation should also increase with stronger filamentation. The characteristics of the radiation can be calculated in the simulations from sample beam particles. This feature [8] is presently being implemented into QuickPIC and OSIRIS [9]. It will be used to determine the best method to detect the radiation in the experiment.

ACKNOWLEDGEMENTS

Work supported by the United States Department of Energy under contract DE-FG02-93ER40745. Simulations are performed on the computers of the USC High Performance Computer Center.

REFERENCES

- [1] T. Piran, Physics Reports, Volume 314, Issue 6 (1999)
- [2] Sentoku et al., Phys. Rev. Lett. 90, 155001 (2003)
- [3] Bret et al., Phys. Rev. Lett. 94, 115002 (2005)
- [4] E. Kallos et al., Phys. Rev. Lett. 100, 074802 (2008)
- [5] Huang et. al., Journal of Computational Physics 217 (2006) 658-679.
- [6] L. Silva et. al - Phys. of Plasmas 9, 2458 (2002)
- [7] W.D. Kimura et. al, AIP Conference Proceedings Volume 877, 534
- [8] L. Silva, private communication
- [9] R.A. Fonseca et. al., Lec. Notes in Computer Science, Vol 2331 (2002)